2011 American Control Conference
on O'Farrell Street, San Francisco, CA, USA
June 29 - July 01, 2011

Determination of All Stabilizing Fractional-Order PID Controllers

Yung K. Lee and John M. Watkins, *Senior Member, IEEE*

Abstract — **A new method for finding all fractional-order (FO) proportional-integral-derivative (PID) controllers that stabilize a given system of integer or non-integer order is proposed. The stability boundaries of such FO PID controllers are calculated in the frequency domain and are given in terms of the proportional gain K_p, integral gain K_i, and derivative gain K_d. In this paper, they will be plotted on the (K_p, K_i), (K_p, K_d), and (K_i, K_d) planes. A key advantage of this approach is that it provides the stability boundaries even when the transfer function of a system is not available, as long as the frequency response of the system can be obtained. Moreover, the method does not require complicated mathematical calculations. An example is presented to illustrate the effectiveness of this method. The results are compared with those of conventional integer-order (IO) PID controllers for a sample example.**

I. Introduction

DESPITE its comparatively long history of more than three hundred years [1], fractional calculus has largely remained a topic of pure mathematics. This is starting to change. In [2], for example, applications of fractional calculus to the fields of physics and engineering, including nonlinear control and fractional order controllers, are explored.

Though PID controllers are clearly in the mainstream of the process control field, their non-integer order counterparts, so called $PI^{\lambda}D^{\mu}$ controllers (where λ and μ are arbitrary real numbers) are starting to receive considerable attention. While integer-order (IO) mathematical models are easier to work with, real physical systems are often described more accurately through non-integer order models. In [3], a torsional system consisting of a rigid disk and a flexible shaft attached thereto was modeled using a fractional-order (FO) transfer function. The resulting frequency response shows that the mechanical resonance effect is represented more naturally with an FO model than an IO model. A simpler form of an FO PID controller, or so called FO PID^k controller (where k is any real number), was used in a control system to suppress a torsional system's backlash vibration in [4]. The French control team CRONE (Controle Robuste d'Ordre Non-Entier) has also been deeply involved in the application of FO controllers to suspension control [5] and flexible transmission [6] of vehicles.

Manuscript received September 22, 2010.

Yung K. Lee is with the Electrical Engineering and Computer Science Department, Wichita State University, Wichita, KS 67260 USA (e-mail: yxlee1@wichita.edu).

John M. Watkins is with the Electrical Engineering and Computer Science Department, Wichita State University, Wichita, KS 67260 USA (e-mail: john.watkins@wichita.edu).

As in the case of IO PID controllers, the stability boundary of an FO PID controller is an important research topic and has received significant attention. In [7], the D-partition method proposed by Neimark in [8] and [9], which has been used for parameter space design of IO controllers, was used to find stability bounds of FO PI or PI^{λ} controllers for four cases. These cases include all combinations of an IO/FO plant and an IO/FO controller. However, only a first order IO plant or an FO plant with order α (where $0<\alpha<1$) was considered.

In [10], the D-decomposition method was used for $PI^{\lambda}D^{\mu}$ controllers that stabilize a given FO system with time delay. For the closed-loop FO characteristic equation, the boundaries of the stability region described by real root boundaries (RRB), infinite root boundaries (IRB) and complex root boundaries (CRB) were determined using the D-decomposition method. In particular, RRB, IRB and CRB provide a general stability region in (K_p, K_i) plane for fixed values of K_d, λ and μ. Unfortunately, solutions in the (K_p, K_d) plane and the (K_i, K_d) plane were not considered. The (K_p, K_d) plane is important if you are considering a PD controller. The (K_i, K_d) plane is important because for certain forms of PID controllers it allows the user to easily determine the values of K_p that will produce stabilizing controllers.

Thus, there exists a need for a more efficient and less complicated way of finding all IO or FO PID controllers that stabilize a given system with an IO or FO transfer function. In [11], the frequency response was used to find all stabilizing IO PID controllers for a given plant transfer function of an arbitrary order. The stabilizing controllers that lie within the stability regions were plotted in three different planes: (K_p, K_i), (K_p, K_d) and (K_d, K_i). However, [11] dealt with an IO PID controller only and the results obtained as such were not applicable to more complicated FO controllers with extra degrees of freedom.

In this paper, a new method for finding all stabilizing $PI^{\lambda}D^{\mu}$ controllers for a given plant transfer function of any order is presented. This method does not require the plant parameters or complicated or time-consuming processes to find all the stabilizing $PI^{\lambda}D^{\mu}$ controllers. The stabilizing $PI^{\lambda}D^{\mu}$ controllers are represented in all three planes of the K_p, K_i and K_d parameter spaces. A detailed mathematical derivation, results, and examples follow.

II. Determination of Stabilizing Controllers

A. Problem Formulation

Consider the unity feedback control system shown in Fig. 1.

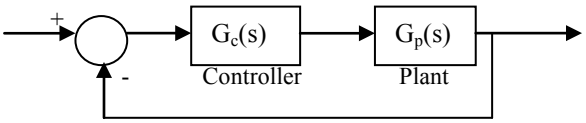

Fig. 1. Control system with negative unity feedback

The plant transfer function is $G_p(s)$ and the transfer function of the $PI^{\lambda}D^{\mu}$ controller $G_c(s)$ is given by

$$G_c(s) = K_p + \frac{K_i}{s^{\lambda}} + K_d s^{\mu} \tag{1}$$

where K_p, K_i and K_d denote the proportional, integral and derivative gains, respectively, and λ and μ are arbitrary positive real numbers.

To determine all the stabilizing $PI^{\lambda}D^{\mu}$ controllers for the given plant, the K_p, K_i and K_d values can be found such that the close-loop characteristic polynomial $\Delta(s)$ of the system shown in Fig. 1 is Hurwitz stable. By determining all the values of the parameters K_p, K_i and K_d that put the closed-loop system poles on the $j\omega$ axis, which represents the marginal stability of the closed-loop system, all the stabilizing $PI^{\lambda}D^{\mu}$ controllers can be found. For marginal stability, the characteristic equation is expressed in the frequency domain by replacing s with $j\omega$.

$$\Delta(j\omega) = 1 + G_p(j\omega)G_c(j\omega) = 0 \tag{2}$$

The plant transfer function $G_p(j\omega)$ can be decomposed into real and imaginary parts as follows:

$$G_p(j\omega) = R_p(\omega) + jI_p(\omega) \tag{3}$$

Then, the characteristic equation (2) becomes

$$\Delta(j\omega) = 1 + \left(R_p(\omega) + jI_p(\omega)\right)\left(K_p + \frac{K_i}{(j\omega)^{\lambda}} + K_d(j\omega)^{\mu}\right) = 0 \tag{4}$$

For (4), the following formula in fractional calculus is used:

$$j^{\lambda} = e^{j(\frac{\pi}{2})\lambda} = \cos(\frac{\pi}{2}\lambda) + j\sin(\frac{\pi}{2}\lambda) \tag{5}$$

Thus,

$$\begin{aligned} &K_p + \frac{K_i}{(j\omega)^{\lambda}} + K_d(j\omega)^{\mu} \\ &= K_p + \frac{K_i}{\omega^{\lambda}}\{\cos(\frac{\pi}{2}\lambda) - j\sin(\frac{\pi}{2}\lambda)\} \\ &\quad + K_d\omega^{\mu}\{\cos(\frac{\pi}{2}\mu) + j\sin(\frac{\pi}{2}\mu)\} \end{aligned} \tag{6}$$

Expanding the characteristic equation in (4) and writing it in terms of its real and imaginary parts yields

$$\Delta(j\omega) = R_{\Delta}(\omega) + jI_{\Delta}(\omega) = 0 \tag{7}$$

where

$$\begin{aligned} R_{\Delta}(\omega) &= 1 + K_p R_p(\omega) \\ &\quad + \frac{1}{\omega^{\lambda}}\{\cos(\frac{\pi}{2}\lambda)R_p(\omega) + \sin(\frac{\pi}{2}\lambda)I_p(\omega)\}K_i \\ &\quad + \omega^{\mu}\{\cos(\frac{\pi}{2}\mu)R_p(\omega) - \sin(\frac{\pi}{2}\mu)I_p(\omega)\}K_d \end{aligned} \tag{8}$$

$$\begin{aligned} I_{\Delta}(\omega) &= K_p I_p(\omega) \\ &\quad + \frac{1}{\omega^{\lambda}}\{\cos(\frac{\pi}{2}\lambda)I_p(\omega) - \sin(\frac{\pi}{2}\lambda)R_p(\omega)\}K_i \\ &\quad + \omega^{\mu}\{\cos(\frac{\pi}{2}\mu)I_p(\omega) + \sin(\frac{\pi}{2}\mu)R_p(\omega)\}K_d \end{aligned} \tag{9}$$

Setting the real and imaginary parts equal to zero gives:

$$\omega^{\lambda}R_p(\omega)K_p + X_{Ri}K_i + X_{Rd}K_d = -\omega^{\lambda} \tag{10}$$

$$\omega^{\lambda}I_p(\omega)K_p + X_{Ii}K_i + X_{Id}K_d = 0 \tag{11}$$

where

$$\begin{aligned} X_{Ri} &= \cos(\frac{\pi}{2}\lambda)R_p(\omega) + \sin(\frac{\pi}{2}\lambda)I_p(\omega) \\ X_{Rd} &= \omega^{\lambda+\mu}\left(\cos(\frac{\pi}{2}\mu)R_p(\omega) - \sin(\frac{\pi}{2}\mu)I_p(\omega)\right) \\ X_{Ii} &= -\sin(\frac{\pi}{2}\lambda)R_p(\omega) + \cos(\frac{\pi}{2}\lambda)I_p(\omega) \\ X_{Id} &= \omega^{\lambda+\mu}\left(\sin(\frac{\pi}{2}\mu)R_p(\omega) + \cos(\frac{\pi}{2}\mu)I_p(\omega)\right) \end{aligned}$$

B. Solution in (K_p, K_i) Plane

This is a three dimensional system in terms of the controller parameters K_p, K_i and K_d. First, we will fix the value of K_d to find the stability region in the (K_p, K_i) plane. In order to deal with two unknowns K_p and K_i, (10) and (11) are rearranged as:

$$\begin{bmatrix} \omega^{\lambda}R_p(\omega) & X_{Ri} \\ \omega^{\lambda}I_p(\omega) & X_{Ii} \end{bmatrix}\begin{bmatrix} K_p \\ K_i \end{bmatrix} = \begin{bmatrix} -X_{Rd}K_d - \omega^{\lambda} \\ -X_{Id}K_d \end{bmatrix} \tag{12}$$

Solving (12) for $\omega \neq 0$ and $\lambda \neq 2n$ (where n is an integer), K_p and K_i are given by

$$K_p = -K_d\omega^{\mu}\frac{\sin\left(\frac{\pi}{2}(\lambda+\mu)\right)}{\sin(\frac{\pi}{2}\lambda)} - \frac{R_p(\omega) - \cot(\frac{\pi}{2}\lambda)I_p(\omega)}{\left|G_p(j\omega)\right|^2} \tag{13}$$

$$K_i = K_d\omega^{\lambda+\mu}\frac{\sin(\frac{\pi}{2}\mu)}{\sin(\frac{\pi}{2}\lambda)} - \frac{\omega^{\lambda}I_p(\omega)}{\sin(\frac{\pi}{2}\lambda)\left|G_p(j\omega)\right|^2} \tag{14}$$

where

$$\left|G_p(j\omega)\right|^2 = R_p{}^2(\omega) + I_p{}^2(\omega) \tag{15}$$

If ω=0, then K_i=0 is implied to define a legitimate PI$^\lambda$D$^\mu$ controller as in (1), which in turn leads to a PD$^\mu$ controller. Such a case will be addressed in the following subsection C with the (K_p, K_d) Plane. Thus, $\omega\neq0$ is assumed in the (K_p, K_i) plane.

If $\lambda=2n$, then the solution exists for the following two cases:

i) For $\mu\neq2n$ and any frequency ω_i that satisfies

$$K_d = \frac{I_p(\omega_i)}{\omega_i{}^\mu \sin(\frac{\pi}{2}\mu)\left|G_p(j\omega_i)\right|^2} \tag{16}$$

the solution for K_i is given in terms of K_p as

$$K_i = -\frac{\omega_i{}^\lambda}{\cos(\frac{\pi}{2}\lambda)}\left(K_p + \frac{\sin(\frac{\pi}{2}\mu)R_p(\omega_i) + \cos(\frac{\pi}{2}\mu)I_p(\omega_i)}{\sin(\frac{\pi}{2}\mu)\left|G_p(j\omega_i)\right|^2}\right) \tag{17}$$

ii) For $\mu=2n$ and any frequency ω_k that satisfies

$$I_p(\omega_k) = 0 \tag{18}$$

the solution for K_i is given in terms of K_p for a fixed K_d value as

$$K_i = -\frac{\omega_k{}^\lambda}{\cos(\frac{\pi}{2}\lambda)}\left(K_p + \omega_k{}^\mu \cos(\frac{\pi}{2}\mu)K_d + \frac{1}{R_p(\omega_k)}\right) \tag{19}$$

Thus, the stability boundary of all stabilizing PI$^\lambda$D$^\mu$ controllers for a fixed K_d value can be found by plotting a two-dimensional graph using the above results, with K_p and K_i as two Cartesian axes. This procedure will be described in detail through an example given in Section III. In addition, for $\lambda=\mu=1$, which is a conventional IO PID controller, the above results reduce to those presented in [11].

C. Solution in (K_p, K_d) Plane

Next, in order to find the stability region in the (K_p, K_d) plane, we will fix the value of K_i. Then, (10) and (11) can be rewritten as:

$$\begin{bmatrix} \omega^\lambda R_p(\omega) & X_{Rd} \\ \omega^\lambda I_p(\omega) & X_{Id} \end{bmatrix}\begin{bmatrix} K_p \\ K_d \end{bmatrix} = \begin{bmatrix} -X_{Ri}K_i - \omega^\lambda \\ -X_{Ii}K_i \end{bmatrix} \tag{20}$$

Solving (20) for $\omega\neq0$ and $\mu\neq2n$ (where n is an integer), K_p and K_d are given by

$$K_p = -K_i\frac{\sin\left(\frac{\pi}{2}(\lambda+\mu)\right)}{\omega^\lambda \sin(\frac{\pi}{2}\mu)} - \frac{R_p(\omega) + \cot(\frac{\pi}{2}\mu)I_p(\omega)}{\left|G_p(j\omega)\right|^2} \tag{21}$$

$$K_d = K_i\frac{\sin(\frac{\pi}{2}\lambda)}{\omega^{\lambda+\mu}\sin(\frac{\pi}{2}\mu)} + \frac{I_p(\omega)}{\omega^\mu \sin(\frac{\pi}{2}\mu)\cdot\left|G_p(j\omega)\right|^2} \tag{22}$$

If ω=0, then K_i=0 as discussed above in subsection B, leading to the following two cases:

i) If $I_p(0)$=0 (typical for real plants),

$$K_p = \frac{-1}{R_p(0)} \tag{23}$$

ii) No solution exists for K_p and K_d otherwise.

If μ =2n and $\omega\neq0$, then the solution exists for the following two cases:

i) For $\lambda\neq2n$ and any frequency ω_i that satisfies

$$K_i = -\frac{\omega^\lambda I_p(\omega_i)}{\sin(\frac{\pi}{2}\lambda)\left|G_p(j\omega_i)\right|^2} \tag{24}$$

the solution for K_d is given in terms of K_p as

$$K_d = -\frac{1}{\omega^\mu \cos(\frac{\pi}{2}\mu)} \times\left(K_p + \frac{\sin(\frac{\pi}{2}\lambda)R_p(\omega) - \cos(\frac{\pi}{2}\lambda)I_p(\omega)}{\sin(\frac{\pi}{2}\lambda)\left|G_p(j\omega)\right|^2}\right) \tag{25}$$

ii) For $\lambda=2n$ and any frequency ω_k that satisfies

$$I_p(\omega_k) = 0 \tag{26}$$

the solution for K_d is given in terms of K_p for a fixed K_i value as

$$K_d = -\frac{1}{\omega_k{}^\mu \cos(\frac{\pi}{2}\mu)}\left(K_p + \frac{\cos(\frac{\pi}{2}\lambda)}{\omega_k{}^\lambda}K_i + \frac{1}{R_p(\omega_k)}\right) \tag{27}$$

Therefore, the stability boundary of all stabilizing PI$^\lambda$D$^\mu$ controllers for a fixed K_i value can be found by plotting a two-dimensional graph using the above results, with K_p and K_d as two Cartesian axes. Again, this procedure will be described in detail through an example given in Section III. For $\lambda=\mu=1$, which is a conventional IO PID controller, the above results reduce to those presented in [11].

D. Solution in (K_i, K_d) Plane

Lastly, we will fix the value of K_p in order to determine the stability region in the (K_i, K_d) plane. Then, (10) and (11) can be rewritten as:

$$\begin{bmatrix} X_{Ri} & X_{Rd} \\ X_{Ii} & X_{Id} \end{bmatrix} \begin{bmatrix} K_i \\ K_d \end{bmatrix} = \begin{bmatrix} -\omega^{\lambda} R_p(\omega) K_p - \omega^{\lambda} \\ -\omega^{\lambda} I_p(\omega) K_p \end{bmatrix} \tag{28}$$

Solving (28) for $\omega \neq 0$ and $\lambda+\mu \neq 2n$ (where n is an integer), K_i and K_d are given by

$$\begin{aligned} K_i = & -K_p \omega^{\lambda} \frac{\sin(\frac{\pi}{2}\mu)}{\sin\left(\frac{\pi}{2}(\lambda+\mu)\right)} \\ & - \frac{\omega^{\lambda}\left(\sin(\frac{\pi}{2}\mu) R_p(\omega) + \cos(\frac{\pi}{2}\mu) I_p(\omega)\right)}{\sin\left(\frac{\pi}{2}(\lambda+\mu)\right)\left|G_p(j\omega)\right|^2} \end{aligned} \tag{29}$$

$$\begin{aligned} K_d = & -\left(\frac{K_p}{\omega^{\mu}}\right) \frac{\sin(\frac{\pi}{2}\lambda)}{\sin\left(\frac{\pi}{2}(\lambda+\mu)\right)} \\ & - \frac{\left(\sin(\frac{\pi}{2}\lambda) R_p(\omega) - \cos(\frac{\pi}{2}\lambda) I_p(\omega)\right)}{\omega^{\mu} \sin\left(\frac{\pi}{2}(\lambda+\mu)\right)\left|G_p(j\omega)\right|^2} \end{aligned} \tag{30}$$

In the (K_i, K_d) plane, $\omega \neq 0$ is assumed without loss of generality as discussed above.

If $\lambda+\mu=2n$ (where n is an integer), the solution exists for the following two cases:

i) For $\lambda \neq 2n$ and any frequency ω_i that satisfies

$$K_p = \frac{\cot(\frac{\pi}{2}\lambda) I_p(\omega_i) - R_p(\omega_i)}{\left|G_p(j\omega_i)\right|^2} \tag{31}$$

the solution for K_d is given in terms of K_i as

$$\begin{aligned} K_d = & \frac{\sin(\frac{\pi}{2}\lambda) R_p(\omega_i) - \cos(\frac{\pi}{2}\lambda) I_p(\omega_i)}{\omega_i^{\lambda+\mu}\left(\sin(\frac{\pi}{2}\mu) R_p(\omega_i) + \cos(\frac{\pi}{2}\mu) I_p(\omega_i)\right)} \\ & \times \left(K_i + \frac{\omega^{\lambda} I_p(\omega_i)}{\sin(\frac{\pi}{2}\lambda)\left|G_p(j\omega_i)\right|^2} \right) \end{aligned} \tag{32}$$

ii) For $\lambda=2n$ and any frequency ω_k that satisfies

$$I_p(\omega_k) = 0 \tag{33}$$

the solution for K_d is given in terms of K_i for a fixed K_p value as

$$K_d = -\frac{1}{\omega_k^{\mu} \cos(\frac{\pi}{2}\mu)} \left(\frac{\cos(\frac{\pi}{2}\lambda)}{\omega_k^{\lambda}} K_i + K_p + \frac{1}{R_p(\omega_k)} \right) \tag{34}$$

Similarly, the stability boundary of all stabilizing PI$^{\lambda}$D$^{\mu}$ controllers for a fixed K_p value can be found by plotting a two-dimensional graph using the above results, with K_i and K_d as two Cartesian axes. This procedure will be described in detail through an example given below. For $\lambda=\mu=1$, which is a conventional IO PID controller, the above results reduce to those presented in [11].

It should be noted that all the results in this section are expressed in the frequency domain. As a consequence, the stability region in the controller parameter space can be determined directly from an experimental frequency response when either the system transfer function or system parameters are unknown.

III. Example

A. Problem Formulation

Consider the following non-minimum phase plant with a second order transfer function having a time delay of 0.8 seconds

$$G_p(s) = \frac{4s+1}{s^2+0.4s+6} e^{-0.8s} \tag{35}$$

The objective here is to find the stability boundaries of all the stabilizing FO PID controllers for the plant transfer function (35) and compare them with those of an IO PID controller. The results will be verified using step responses. In this example, an FO PID controller with $\lambda=1.0$ and $\mu=0.5$ is used for the controller transfer function in (1). Thus, the PI$^{\lambda}$D$^{\mu}$ controller used is given by

$$G_c(s) = K_p + \frac{K_i}{s} + K_d s^{0.5} \tag{36}$$

B. Comparative Results in (K_p, K_i) Plane

In order to find the stability region in the (K_p, K_i) plane for the plant transfer function (35) and the PI$^{\lambda}$D$^{\mu}$ controller transfer function (36) with a fixed value $K_d=0.6$, (13) and (14) were used. In Fig. 2, the stability regions of the IO and FO PID controllers are plotted in the (K_p, K_i) plane. In this figure, the area enclosed by the dashed line is the stability region for the FO PID controller, and the area enclosed by the solid line is the stability region for the IO PID controller. The same applies to Fig. 4 as well. As can be seen, the FO PID controller provides a fairly wide stability region, whereas the IO PID controller does not provide any stability region for $K_d=0.6$.

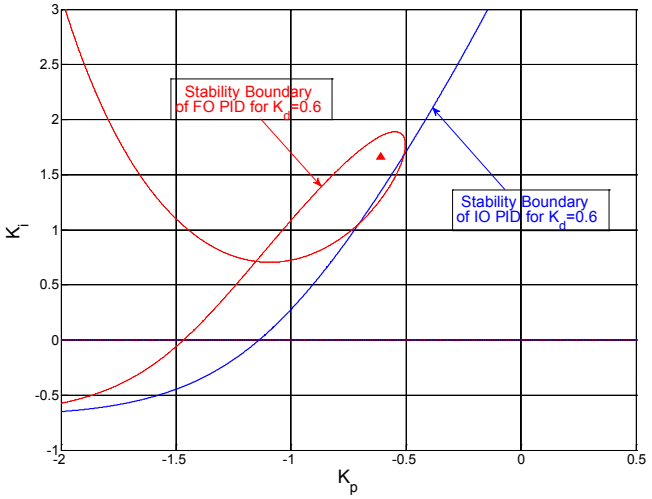

Fig. 2. Stability regions in (K_p, K_i) plane for K_d=0.6

An arbitrary controller was chosen from the stability region of the FO PID controller in Fig. 2, which is K_p= -0.6089 and K_i=1.6608 as marked on the plot. Accordingly, the FO PID controller found is given by

$$G_{cFO}(s) = -0.6089 + \frac{1.6608}{s} + 0.6s^{0.5} \tag{37}$$

Fig. 3 shows the corresponding closed-loop step response with the above FO PID controller. In the example, the closed-loop system with the FO PID controller (37) has a percent overshoot of P.O=11% and a 2% settling time of t_s=22.7 seconds.

To determine the closed-loop step response of the FO PID controller (37), the FO PID controller transfer function is approximated using the fractional power pole (FPP) and fractional power zero (FPZ) methods given in [12] and [13], respectively.

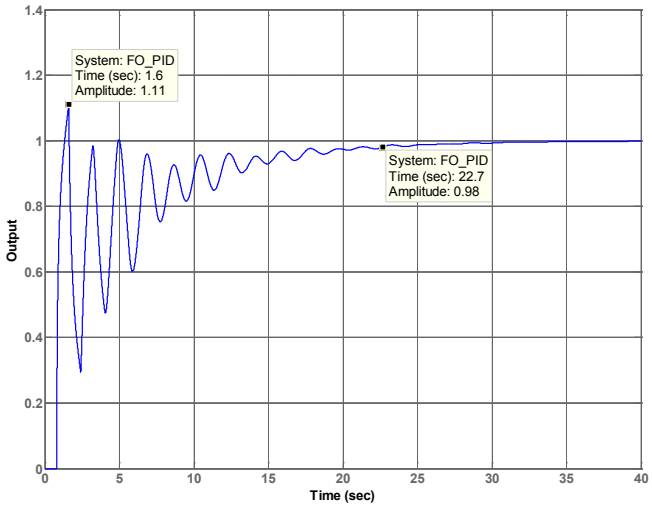

Fig. 3. Closed-loop step response with the FO PID controller for K_d=0.6

C. Comparative Results in (K_p, K_d) Plane

In a similar way, to find the stability region in the (K_p, K_d) plane for the plant transfer function (35) and the PI$^{\lambda}$D$^{\mu}$ controller transfer function (36) with a fixed value K_i=1.2, (21) and (22) were used. In Fig. 4, the stability regions of the IO and FO PID controllers are plotted in the (K_p, K_d) plane for K_i=1.2. As can be seen, the FO PID controller provides a wider stability region than the IO PID controller does.

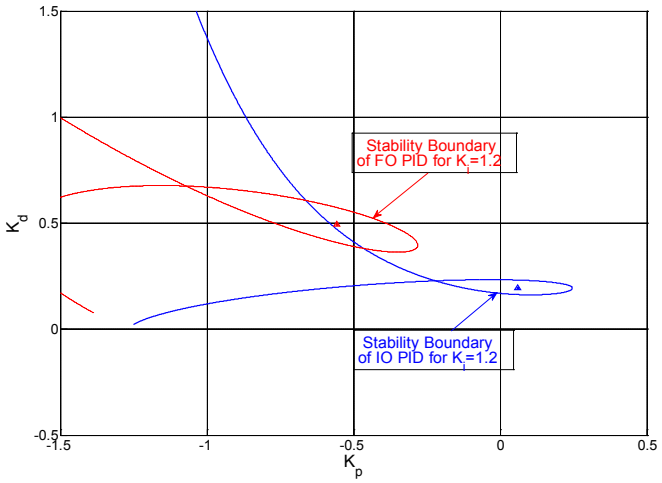

Fig. 4. Stability regions in (K_p, K_d) plane for fixed K_i=1.2

As marked on the plot, two arbitrary controllers were chosen from the stability regions in Fig. 4. For the IO PID, K_p=0.0595 and K_d=0.1955 were chosen and for the FO PID, K_p= -0.5575 and K_d=0.4948 were chosen. Accordingly, the IO PID controller found is given by

$$G_{cIO}(s) = 0.0595 + \frac{1.2}{s} + 0.1955s \tag{38}$$

and the FO PID controller found is given by

$$G_{cFO}(s) = -0.5575 + \frac{1.2}{s} + 0.4948s^{0.5} \tag{39}$$

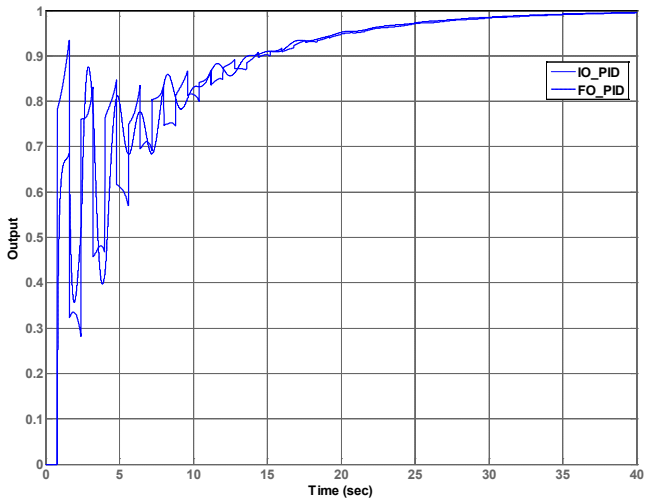

Fig. 5. Closed-loop step responses with the IO and FO PID controllers for K_i =1.2

D. Comparative Results in (K_i, K_d) Plane

Lastly, (29) and (30) were used to find the stability region in the (K_i, K_d) plane for the plant transfer function (35) and the $PI^{\lambda}D^{\mu}$ controller transfer function (36) with a fixed value K_p=-0.8. In Fig. 6, the stability regions of the IO and FO PID controllers are plotted in the (K_i, K_d) plane. In the figure, the area enclosed by the dashed line and K_i=0 is the stability region for the FO PID controller, and the area enclosed by the solid line and K_i=0 is the stability region for the IO PID controller. As can be seen from the plot, the FO PID controller provides a stability region enclosed by two curves and a line K_i=0; however, the IO PID controller does not provide any stability region in this case.

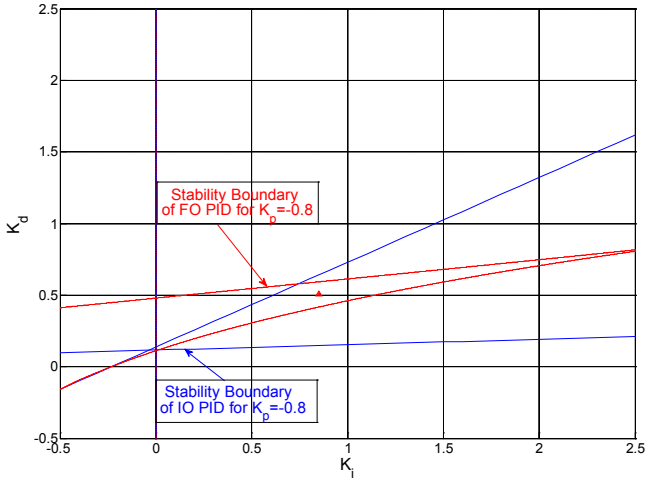

Fig. 6. Stability regions in (K_i, K_d) plane for K_p =-0.8

Next, an arbitrary controller is chosen from the stability region of the FO PID controller in Fig. 6, which is K_i=0.8503 and K_d=0.5084 as marked on the plot. Accordingly, the FO PID controller found is given by

$$G_{cFO}(s) = -0.8 + \frac{0.8503}{s} + 0.5084 s^{0.5} \qquad (40)$$

Fig. 7 shows the corresponding closed-loop step response with the above FO PID controller (40). In this example, the closed-loop system with the FO PID controller (40) has a 2% settling time of t_s=34.6 seconds and no percent overshoot.

IV. Conclusion

As described in Sections II and III, a new method for determining all stabilizing $PI^{\lambda}D^{\mu}$ controllers for a given system is presented. Since the method is fundamentally based on the frequency response of a system, this method can be applied even when the system parameters are not known. In addition, the results shown in Section III are promising because for this example an FO PID controller provides stability regions even when an IO PID controller cannot provide any stability region and the FO PID controller provides a much larger stability region than the IO PID controller does when the IO PID controller provides a stability region, which in turn gives more flexibility when designing a controller. This is not surprising as an IO PID controller is a special case of an FO PID controller.

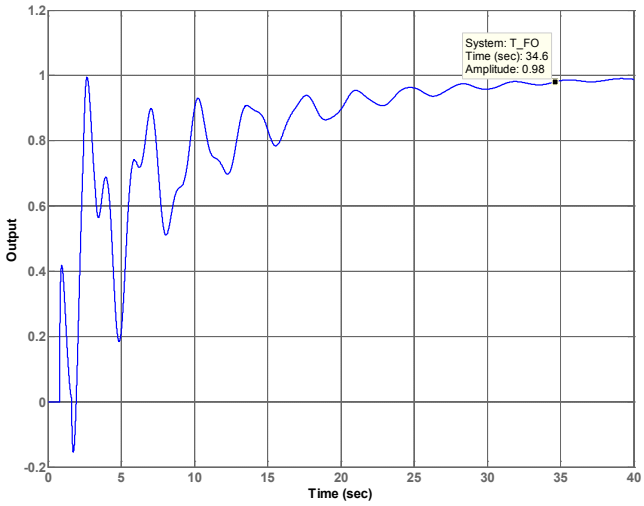

Fig. 7. Closed-loop step response with the FO PID controller for K_p=-0.8.

References

[1] K. B. Oldham and J. Spanier, *The Fractional Calculus*. New York: Academic Press, 1974.

[2] R. Hilfer (Ed.), *Applications of Fractional Calculus in Physics*. Singapore: World Scientific, 2001.

[3] S. Manabe, "A suggestion of fractional-order controller for flexible spacecraft attitude control," *Nonlinear Dynamics*, vol. 29, no.1-4, pp.251-268, 2002.

[4] C. Ma and Y. Hori, "Backlash vibration suppression control of torsional system by novel fractional order PIDk controller," *IEEJ Trans. Ind. Applicat.*, vol. 124-D, no.3, pp. 312-317, 2004.

[5] A. Oustaloup, X. Moreau, and M. Nouillant, "The CRONE suspension," *Control Eng. Practice*, vol. 4, no. 8, pp. 1101-1108, 1996.

[6] A. Oustaloup, B. Mathieu, and P. Lanusse, "The CRONE control of resonant plants: Application to a flexible transmission," *Eur. J. Contr.*, vol. 1, no. 2, pp. 113-121, 1995.

[7] A. Ruszewski, "Stability regions of closed loop system with time delay inertial plant of fractional order and fractional order PI controller," *Bulletin of the Polish Academy of Sciences, Technical Sciences*, vol. 56, no. 4, 2008.

[8] J. Neimark, "D-subdivisions and spaces of quasi-polynomials," *Prikl. Mat. Meth.*, vol. 13, pp.349-380, 1949.

[9] Y. I. Neimark, "Robust stability and D-partition," *Automation and Remote Control* 53 (1992) (7), pp.957-965.

[10] S. E. Hamamci, "An algorithm for stabilization of fractional-order time delay systems using fractional-order PID controllers," *IEEE Transactions on Automatic Control,* vol. 52, no. 10, October 2007

[11] S. Sujoldžić and J. M. Watkins, "Stabilization of an arbitrary order transfer function with time delay using a PID controller," *Proceedings of the 45th IEEE Conference on Decision and Control*, San Diego, CA, USA, 2006.

[12] A. Charef, H. H. Sun, Y. Y. Tsao, and B. Onaral, "Fractal system as represented by a singularity function," *IEEE Trans. Autom. Control*, vol. 37, no. 9, pp.1465-1470, 1992.

[13] A. Charef, "Analogue realization of fractional-order integrator, differentiator and fractional $PI^{\lambda}D^{\mu}$ controller," *IEE Proc. Control Theory Appl*. vol. 153, no. 6, November 2006.